Loss of *Frzb* and *Sfrp1* differentially affects joint homeostasis in instability-induced osteoarthritis

Sarah Thysen[1], Frank P. Luyten [2,3], Rik J. Lories [1,3]

[1] Laboratory of Tissue Homeostasis and Disease, Skeletal Biology and Engineering Research Center, Department of Development and Regeneration, KU Leuven, Belgium

[2] Skeletal Biology and Engineering Research Center, Department of Development and Regeneration, KU Leuven, Belgium

[3] Division of Rheumatology, University Hospitals Leuven, Belgium

Author email addresses: Sarah.Thysen@med.kuleuven.be; Frank.Luyten@uz.kuleuven.be; Rik.Lories@uz.kuleuven.be

Corresponding author:

Dr. Rik Lories, Laboratory of Tissue Homeostasis and Disease, SBE Centre, O&N1 – Box 813, Herestraat 49, B3000 Leuven, Belgium. Rik.Lories@uz.kuleuven.be. Phone: +32-16-342541; Fax: + 32-16-342543.

Running title:

SFRPs in OA

Keywords:

Cartilage – Osteoarthritis – Wnt – SFRP – FRZB – Subchondral bone

Abstract

Objective: To investigate the specific role of FRZB and SFRP1 in the onset and progression of OA using *Frzb*$^{-/-}$ and *Sfrp1*$^{-/-}$ mice in the destabilization of medial meniscus model (DMM), a slowly progressing model of OA. Secreted frizzled related proteins (SFRPs) were identified as secreted Wnt antagonists. The Wnt signaling cascade is a major regulator in cartilage development, homeostasis and degeneration.

Methods: The DMM model was surgically induced in eight-week-old male C57/Bl6 *Frzb*$^{-/-}$, *Sfrp1*$^{-/-}$ or wild-type mice by transection of the medial meniscotibial ligament. Cartilage damage in the femoral and tibial articular surfaces was calculated following the OARSI histopathology initiative guidelines. Histomorphometry was used to evaluate the subchondral bone plate thickness.

Results: OA severity scores were significantly higher in the tibia of *Frzb*$^{-/-}$ mice as compared to littermates, whereas no interaction was seen between genotype and intervention in *Sfrp1*$^{-/-}$ mice. Moreover, the DMM model resulted in significantly greater subchondral bone changes compared to sham but was not different between *Frzb*$^{-/-}$ mice and littermates. In contrast, the subchondral bone properties in *Sfrp1*$^{-/-}$ mice were significantly different from littermates

Conclusion: Using the DMM model, we demonstrated that FRZB and SFRP1 differentially modulate joint homeostasis in two distinct compartments of the joint. These data highlight the fine-tuning of Wnt signaling in joint homeostasis and disease, show differential regulation of the cascade in cartilage and subchondral bone, and provide further evidence for a role of endogenous Wnt modulators as key players in OA.

Introduction

Osteoarthritis (OA) is a chronic and progressive joint disorder characterized by structural damage to one or more joints. Symptoms vary from mild to severe joint pain and stiffness, often leading to loss of joint function and permanent disability. Genetic as well as acquired factors, including trauma and life-style associated features such as obesity contribute to the disease. OA is considered a disease of the whole joint: in addition to the articular cartilage, the subchondral bone and synovium also play important roles in onset and progression of OA. In early stages cell proliferation and enhanced matrix remodeling occur simultaneously in both cartilage and bone. When the balance between anabolic and catabolic processes in the joint is lost, the remodeling response results in articular cartilage degradation, osteophyte formation and subchondral bone sclerosis. The latter is associated with reduced mineralization secondary to increased tissue turnover and leading to impaired bone quality [1].

Polymorphisms in Frizzled-related protein (*FRZB/SFRP3)* have been associated with OA [2], although this has been challenged more recently in genetic studies of very large cohorts [3]. Nevertheless, mice with loss of *Frzb* show increased severity of OA in different acute models [4]. FRZB is a member of the secreted frizzled related protein (SFRP) family, which includes five members (SFRP1-5). SFPRS were originally identified as extracellular ligand-binding inhibitors of the Wingless-type (Wnt) signaling cascade.

More recent data suggest that SFRPs have a broad range of biological activities, including negative and positive modulation of Wnt signaling and additional interactions with molecules that are unrelated to Wnt signaling [5]. The Wnt signaling cascade is a major regulator of the development and growth of bone and cartilage [6]. Finely tuned Wnt signaling is required to maintain the integrity and homeostasis of the bone-cartilage unit. Therefore, disregulation of Wnt signaling can lead to OA development [6-8].

Frzb$^{-/-}$ and *Sfrp1*$^{-/-}$ mice have contrasting skeletal phenotypes: *Frzb*$^{-/-}$ mice show increased cortical thickness without changes in the trabecular bone [4], whereas increased trabecular but normal cortical bone is observed in *Sfrp1* deficient mice [9]. The role of SFRP1 in OA has not been studied. In this study, we therefore investigated the role of both FRZB and SFRP1 in the onset and progression of OA using *Frzb*$^{-/-}$ and *Sfrp1*$^{-/-}$ mice in the destabilization of medial meniscus model (DMM) of OA, a model with relatively slow disease progression offering an excellent translational perspective on OA development.

Materials and methods

Mice

Frzb$^{-/-}$ mice [4] were backcrossed onto the C57BL/6 background for more than 10 generations. *Sfrp1*$^{-/-}$ C57/Bl6 mice were a gift from J. Rubin (Bethesda, MD, USA). These

mice were compared to age matched C57BL/6 littermates. The animals were housed in conventional conditions: 12-h light/dark cycle, standard diet (1% calcium, 0.76% phosphate) and water ad libitum. All experiments were approved by the Ethical Committee for animal research at KU Leuven (P198/2012).

Destabilization of the medial meniscus (DMM) model in mice

The DMM model of OA was surgically induced in the right knee of eight-week-old male *Frzb*$^{-/-}$ (n= 16), *Sfrp1*$^{-/-}$ (n= 10) or wild-type mice (n= 12 and n= 16) by transection of the medial meniscotibial ligament [10]. Sham-operated knees (*Frzb*$^{-/-}$ (n= 13), *Sfrp1*$^{-/-}$ (n= 6) or wild-type mice (n= 13 and n= 18)) were used as control. Eight weeks after surgery, mice were sacrificed and knees were dissected for histology. Knee sections (5 sections, 100 µm apart) were stained with haematoxylin-eosin and Safranin O. Cartilage damage in the femoral and tibial articular surfaces was quantified following the OARSI histopathology initiative guidelines in a blinded fashion [11].

Subchondral bone plate histomorphometry

Histomorphometry was performed on Safranin-O- stained sections using an Olympus DP73 microscope and digital image analysis using Osteomeasure software. First, a box with a fixed width (800 µM) and variable height with the upper limit at the transition of calcified cartilage to subchondral bone and the lower limit at the transition subchondral bone to growth plate was created from the digital image (referred to as subchondral bone area, area defined by blue line in figure II A). Next, a new box with the upper limit

matched to the first box and the lower limit at the transition of the subchondral bone plate to trabecular bone was generated (referred to as subchondral bone plate area, area defined by white line in figure II A). The lined surface areas were calculated using the Osteomeasure software. To correct for variances due to section artifacts, we do not show the subchondral bone plate surface area per se, but express the subchondral bone plate thickness as a ratio of the subchondral bone plate area to the subchondral bone area.

Immunohistochemistry

Procedures and materials used for immunohistochemistry are presented in Supplementary Materials

Statistics

All analyses were performed with GraphPad Prism. We hypothesized that the dependent variables (OA severity and subchondral bone plate thickness) could be determined by two independent variables (genotype and surgery) and therefore tested the effect of genotype, surgical intervention and their interaction using 2-way ANOVA. The assumptions underlying the ANOVA were assessed: the dependent variables were measured at a ratio level and the independent variables were categorical, independent and based on independent observations. For subchondral bone plate analysis, data were normally distributed in the SFRP1 experiment based on visual analysis and the D'Agostino – Pearson omnibus normality test. In the FRZB experiment one outlier was identified by the Grubbs method affecting the normal distribution. Removal of the outlier resulted in a normal distribution assessed as above. 4-group analyses in both

setups suggested homogeneity of variance for both original and cleaned datasets based on the Brown-Forsythe test. For OA severity analysis, data were not normally distributed and there was no homogeneity of variance. We therefore performed a log transformation of the scores resulting in positive assessment of the normal distribution for the different datasets and homogeneity of variance assessed as above. ROUT and Grubbs method did identify outliers in both the FRZB and SFRP1 experiments. 2-way ANOVA was performed on original as well as cleaned datasets. Only the analysis of the original data is reported as removal of outliners emphasized detected differences with smaller 95% confidence intervals of differences between means. If a significant interaction was detected, post-hoc Sidak test taking into account multiple comparisons was applied. Data are presented as mean + 95% CI and p-values < 0.05 were considered significant. In the post-hoc tests, adjusted p-values < 0.05 correspond with 95% CI for differences between means that do not contain the zero value.

Results

To study the role of SFRPs in a slowly progressing model of OA, the DMM model was induced in *Frzb*$^{-/-}$, *Sfrp1*$^{-/-}$ and wild-type mice. 8 weeks after induction, OA severity scores were significantly higher in the tibia of *Frzb*$^{-/-}$ mice as compared to littermates (2-way ANOVA p = 0.0105 for interaction between genotype and intervention – p < 0.05 between *Frzb*$^{-/-}$ and littermates in DMM but not sham intervention with difference

between means respectively -0.431 (95CI: -0.838;-0.024) for DMM and 0.254 (95%CI: -0.18;0.687) for Sham (Sidak test). For the femur overall scoring was lower compared to tibia. DMM mice had significantly higher scores than sham operated animals, but there was no interaction with the specific genotype. These data correspond with the OARSI position paper [11] indicating that the scoring of the femoral condyle is more challenging due to thinner cartilage, the definition of the tidemark and the convex shape of the condyles, hence leading to lower overall scores and larger error margins.

For the *Sfrp1*$^{-/-}$ mice as compared to littermates no interaction between genotype and intervention was seen at either the tibia or femur (figure I).

We measured the subchondral bone plate thickness of the medial tibial plateau of DMM-induced and sham-operated mice by histologic assessment at 8-weeks post surgery. The DMM model resulted in significantly greater subchondral bone changes compared to sham but was not different between *Frzb*$^{-/-}$ mice and littermates ((2-way ANOVA $p < 0.05$ for intervention only). In contrast, the subchondral bone properties in *Sfrp1*$^{-/-}$ mice were significantly different from littermates ((2-way ANOVA $p = 0.04$ for interaction between genotype and intervention) (figure II). Sidak test returned a *p*-value equal to 0.06 for the difference between *Sfrp1*$^{-/-}$ mice and littermates in the DMM model with the difference between means respectively -6,26 (95%CI: -12.79;0.268) for DMM and 3.147 (95%CI -5.189;11.483) for sham.

FRZB immunohistochemical staining indicated the presence of FRZB in the deep layer of the articular cartilage in wild-type mice (Supplementary Figure I A/II A), as previously was also observed for human cartilage [12]. This staining was absent in *Frzb*$^{-/-}$ mice and

appeared reduced in *Sfrp1*$^{-/-}$ mice. We could not observe any Frzb in the subchondral bone of wild-type, *Frzb*$^{-/-}$ and *Sfrp1*$^{-/-}$ mice. Total beta-catenin staining was primarily located in the superficial layers of the articular cartilage (Supplementary Figure I B/II B). The staining suggested that more beta-catenin was present in *Frzb*$^{-/-}$ mice upon DMM surgery compared to sham-operated, whereas the opposite is true for *Sfrp1*$^{-/-}$ mice. These data complement our findings that *Frzb*$^{-/-}$ and *Sfrp1*$^{-/-}$ show different phenotypes upon DMM induction and may suggest that these findings are at least partly due to differences in canonical Wnt signaling. Due to technical limitations we could not achieve successful SFRP1 staining.

Discussion

Using the DMM model, we demonstrate that FRZB and SFRP1 differentially modulate joint homeostasis in two distinct compartments of the joint. These data highlight the relevance of Wnt signaling in joint surface and subchondral bone biology, and provide further evidence for a role of endogenous Wnt modulators as key players in these processes. Earlier *in vivo* data demonstrate that *Frzb*$^{-/-}$ mice are more prone to cartilage damage in different short-term models of OA [4]. Transcriptome analysis of the bone-cartilage unit in joints of *Frzb*$^{-/-}$ mice further revealed that the Wnt pathway is tightly regulated with compensatory upregulation of other Wnt modulators in the absence of Frzb. Moreover, *in vitro* studies highlight the key function for Frzb in cartilage

homeostasis [13]. Although *Frzb*$^{-/-}$ mice are reported with increased cortical bone thickness and density [4], loss of Frzb did not lead to an increase of subchondral bone plate thickness compared to control in the DMM model.

Targeted inactivation of another member of the SFRP family, Sfrp1, did not lead to increased cartilage degeneration upon DMM. However, we could observe thickening of the subchondral bone plate compared to control. The anabolic effect of loss of Sfrp1 on the subchondral bone is consistent with previous *in vivo* data. Genetic deletion of *Sfrp1* increases trabecular bone mass with a reduction in osteoblast and osteocyte apoptosis [14]. *Sfrp1* may also inhibit osteoclastogenesis by binding of nuclear factor-kappaB ligand (RANKL), a ligand that is expressed by osteoblastic cells and promotes osteoclast differentiation through interaction with their cognate signaling receptor RANK [15]. Our data may imply that Sfrp1 plays mainly a role in the subchondral bone and not in the homeostasis of articular cartilage during OA.

Previous studies by Zhu et al. already highlighted how Wnt signaling can affect joint homeostasis with both gain and loss of function for key signaling mediator beta-catenin resulting in osteoarthritis-like phenotypes [7, 8]. Although the SFRP family has originally been identified as extracellular Wnt antagonists, it has become increasingly clear that they should be regarded as Wnt modulators (both in a positive and negative way) and that their interactome extends beyond Wnt ligands [5].

Finally, the differential effects of loss of SFRP1 and FRZB on cartilage and subchondral bone in this model suggest that, at least in the initial phase of disease, cartilage and subchondral bone remodeling may be uncoupled or at least modulated by distinct molecules belonging to the same family. In the context of this study, this could be partly explained by the difference in the expression profile of FRZB and SFRP1. Whereas Frzb is predominantly expressed postnatally in the cartilage and periosteum of mice [4], Sfrp1 expression is observed in cartilage [13] but appears most important in osteoblast differentiation [14]. Taken together this accumulating evidence further highlights the potential of Wnt signaling modulation in the joint as a therapeutic target but at the same time demonstrates the critical role of the microenvironment in determining the outcome of the disease processes.

Acknowledgements

The authors would like to thank Mrs. Ann Hens and Lies Storms for maintaining the mouse colonies and other technical assistance, as well as Prof. Christa Maes for her aid in the analyses of the subchondral bone.

Author contributions

All authors contributed to the conception and design of the study, acquisition, analysis or interpretation of the data. All authors also contributed to drafting and revising the

manuscript and approved the final version to be submitted. R. Lories, as corresponding author, takes responsibility of the integrity of the work as a whole, from inception to finished article.

Role of the funding source

This work was supported by research grant nr. G.0717.09 from the Scientific Research Fund Flanders (FWO Vlaanderen) and an OT grant from KU Leuven to R. Lories. The study sponsors had no direct involvement in the study, in writing of the manuscript or the decision to submit.

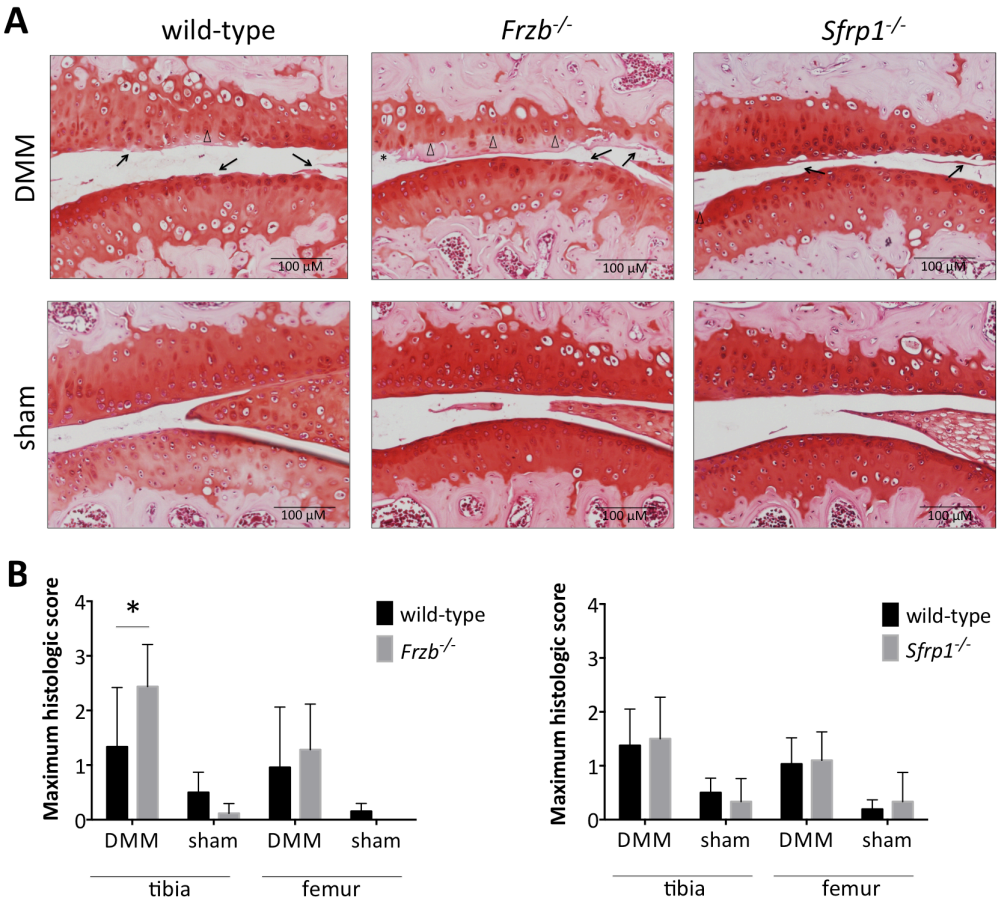

Figure 1. Loss of Frzb increases cartilage damage in DMM model of OA. (A) Representative frontal hematoxylin-Safranin O stained sections of wild-type, *Frzb*$^{-/-}$ and *Sfrp1*$^{-/-}$ knees (medial condyle) in the DMM model or sham operated. Bar= 100 µM, original magnification 20x. Arrows indicate cartilage fibrillation, triangles indicate loss of proteoglycans and asterisks indicate loss of cartilage. (B) Quantification of articular cartilage erosion in wild-type, *Frzb*$^{-/-}$ and *Sfrp1*$^{-/-}$ mice, subjected to either sham or DMM. The medial condyle of tibia and femur were evaluated by the OARSI scoring system. Data are shown as the maximum histologic score + 95% confidence interval. Left: WT sham- operated (n=13), WT DMM (n=12), *Frzb*$^{-/-}$ sham-operated (n=13) and *Frzb*$^{-/-}$ DMM (n=16). 2-way ANOVA $p < 0.05$ for genotype, intervention and interaction – $p < 0.05$ between *Frzb*$^{-/-}$ and littermates (Sidak test). Right: WT sham-operated (n=18), WT DMM (n=16), *Sfrp1*$^{-/-}$ sham-operated (n=6) and *Sfrp1*$^{-/-}$ DMM (n=10).

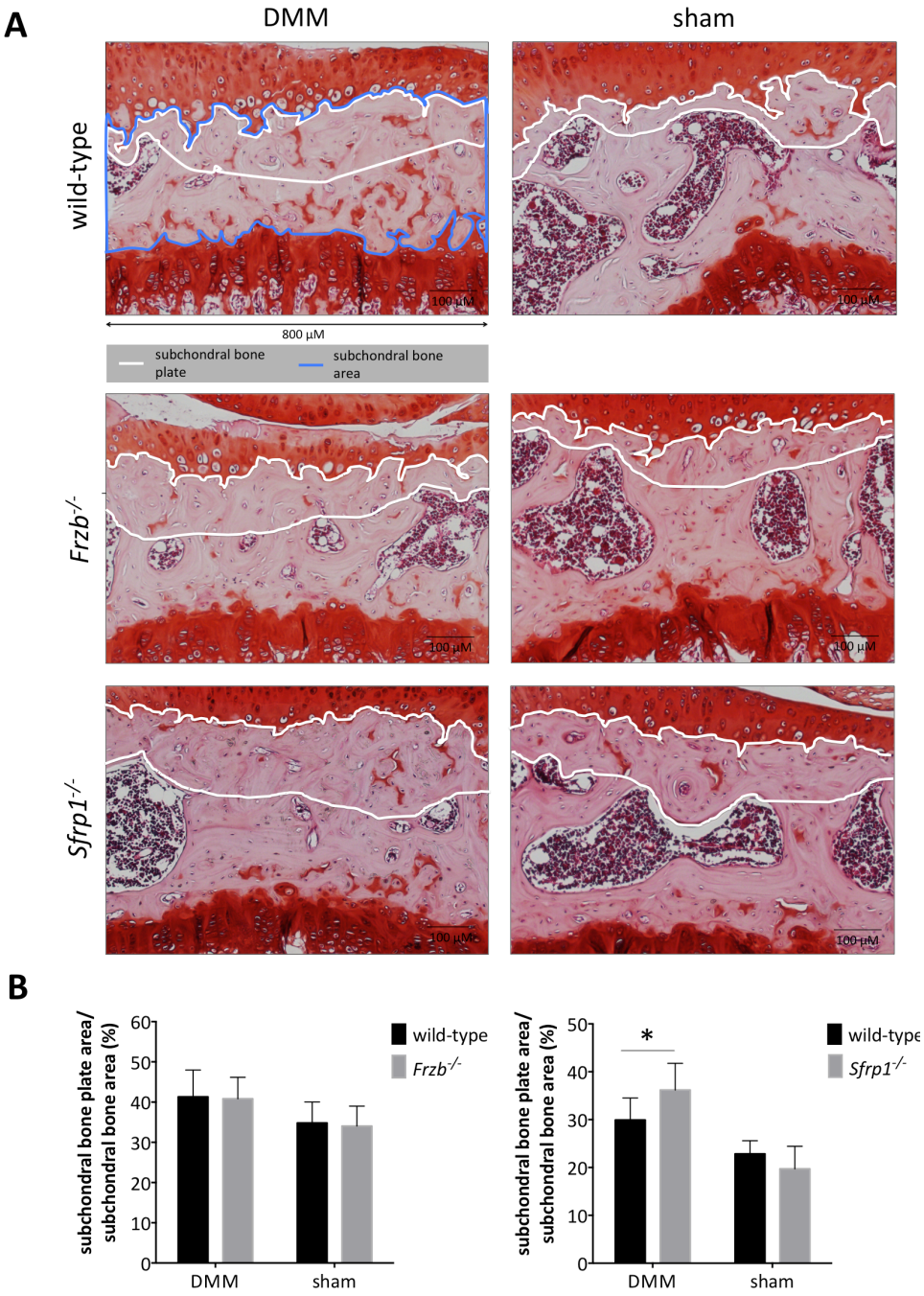

Figure 2. Loss of Sfrp1 increases subchondral bone plate thickness in DMM model of OA. (A) Representative frontal hematoxylin-Safranin O stained sections of wild-type, *Frzb*$^{-/-}$ and *Sfrp1*$^{-/-}$ knees (medial condyle) in the DMM model or sham operated. Blue line delineates the subchondral bone area and white lines delineate the subchondral bone plate thickness. Bar= 100 µM, original magnification 10x. (B) Quantification of the subchondral bone plate. Data are shown as the mean ratio of subchondral bone plate area/ subchondral bone area + 95% confidence interval. Left: WT sham- operated (n=20), WT DMM (n=16), *Frzb*$^{-/-}$ sham-operated (n=12) and *Frzb*$^{-/-}$ DMM (n=13) (2-way ANOVA $p < 0.05$ for intervention only). Right: WT sham- operated (n=20), WT DMM (n=16), *Sfrp1*$^{-/-}$ sham-operated (n=5) and *Sfrp1*$^{-/-}$ DMM (n=11) (2-way ANOVA $p < 0.05$ for intervention and interaction).

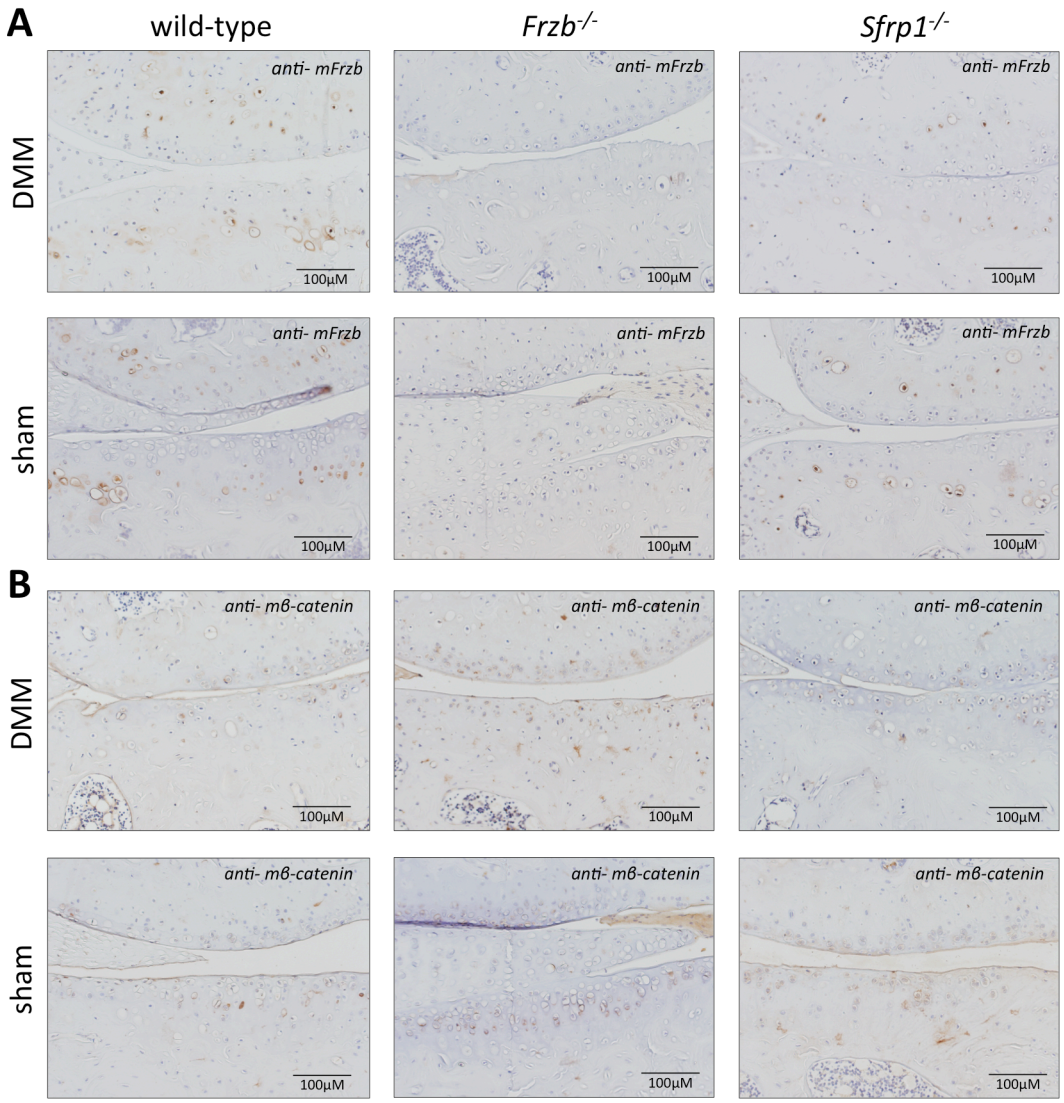

Supplementary Figure 1. Frzb and beta-catenin are present in the articular cartilage. Immunohistochemistry for Frzb (A) and total beta-catenin (B) on frontal sections of wild-type, *Frzb*$^{-/-}$ and *Sfrp1*$^{-/-}$ knees (medial condyle) in the DMM model or sham operated. Bar= 100 µM, original magnification 20x

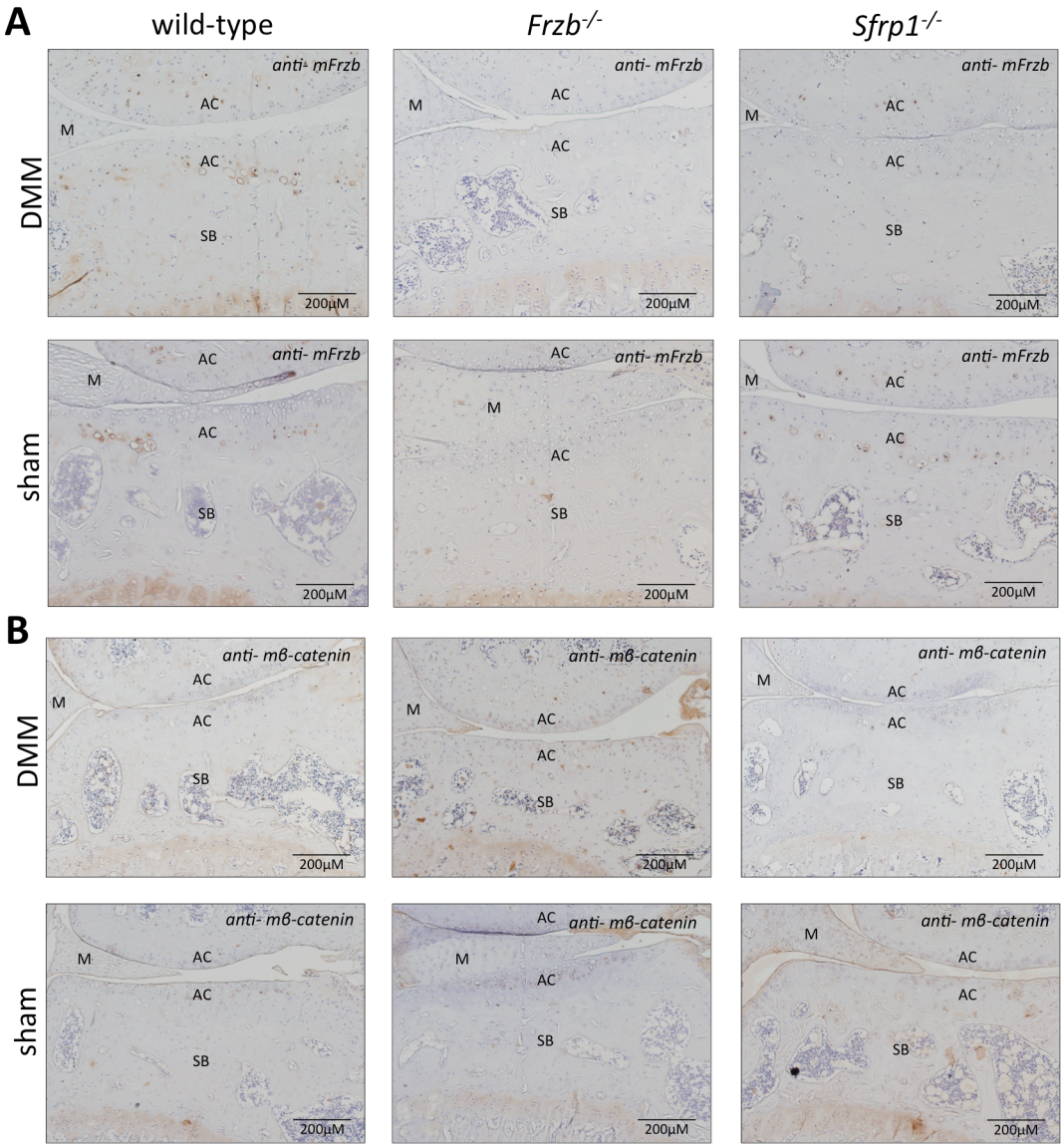

Supplementary Figure 2. Frzb and beta-catenin in the articular cartilage and the subchondral bone. Immunohistochemistry for Frzb (A) and total beta-catenin (B) on frontal sections of wild-type, *Frzb*$^{-/-}$ and *Sfrp1*$^{-/-}$ knees (medial condyle) in the DMM model or sham operated. M, Meniscus. AC, articular cartilage. SB, subchondral bone. Bar= 200 µM, original magnification 10x

References

1. Lories, R.J. and F.P. Luyten, *The bone-cartilage unit in osteoarthritis.* Nat Rev Rheumatol, 2011. **7**(1): p. 43-9.
2. Loughlin, J., et al., *Functional variants within the secreted frizzled-related protein 3 gene are associated with hip osteoarthritis in females.* Proc Natl Acad Sci U S A, 2004. **101**(26): p. 9757-62.
3. Evangelou, E., et al., *Large-scale analysis of association between GDF5 and FRZB variants and osteoarthritis of the hip, knee, and hand.* Arthritis Rheum, 2009. **60**(6): p. 1710-21.
4. Lories, R.J., et al., *Articular cartilage and biomechanical properties of the long bones in Frzb-knockout mice.* Arthritis Rheum, 2007. **56**(12): p. 4095-103.
5. Bovolenta, P., et al., *Beyond Wnt inhibition: new functions of secreted Frizzled-related proteins in development and disease.* J Cell Sci, 2008. **121**(Pt 6): p. 737-46.
6. Lories, R.J., M. Corr, and N.E. Lane, *To Wnt or not to Wnt: the bone and joint health dilemma.* Nat Rev Rheumatol, 2013. **9**(6): p. 328-39.
7. Zhu, M., et al., *Activation of beta-catenin signaling in articular chondrocytes leads to osteoarthritis-like phenotype in adult beta-catenin conditional activation mice.* J Bone Miner Res, 2009. **24**(1): p. 12-21.

8. Zhu, M., et al., *Inhibition of beta-catenin signaling in articular chondrocytes results in articular cartilage destruction.* Arthritis Rheum, 2008. **58**(7): p. 2053-64.

9. Bodine, P.V., et al., *The Wnt antagonist secreted frizzled-related protein-1 is a negative regulator of trabecular bone formation in adult mice.* Mol Endocrinol, 2004. **18**(5): p. 1222-37.

10. Glasson, S.S., T.J. Blanchet, and E.A. Morris, *The surgical destabilization of the medial meniscus (DMM) model of osteoarthritis in the 129/SvEv mouse.* Osteoarthritis Cartilage, 2007. **15**(9): p. 1061-9.

11. Glasson, S.S., et al., *The OARSI histopathology initiative - recommendations for histological assessments of osteoarthritis in the mouse.* Osteoarthritis Cartilage, 2010. **18 Suppl 3**: p. S17-23.

12. Leijten, J.C., et al., *GREM1, FRZB and DKK1 mRNA levels correlate with osteoarthritis and are regulated by osteoarthritis-associated factors.* Arthritis Res Ther, 2013. **15**(5): p. R126.

13. Lodewyckx, L., et al., *Tight regulation of wingless-type signaling in the articular cartilage - subchondral bone biomechanical unit: transcriptomics in Frzb-knockout mice.* Arthritis Res Ther, 2012. **14**(1): p. R16.

14. Bodine, P.V., et al., *The Wnt antagonist secreted frizzled-related protein-1 controls osteoblast and osteocyte apoptosis.* J Cell Biochem, 2005. **96**(6): p. 1212-30.

15. Hausler, K.D., et al., *Secreted frizzled-related protein-1 inhibits RANKL-dependent osteoclast formation.* J Bone Miner Res, 2004. **19**(11): p. 1873-81.